

Vortex quasi-crystals in mesoscopic superconducting samples

Wei Zhang* and C. A. R. Sá de Melo

School of Physics, Georgia Institute of Technology, Atlanta, Georgia 30332

(Dated: November 1, 2018)

There seems to be a one to one correspondence between the phases of atomic and molecular matter (AMOM) and vortex matter (VM) in superfluids and superconductors. Crystals, liquids and glasses have been experimentally observed in both AMOM and VM. Here, we propose a vortex quasi-crystal state which can be stabilized due to boundary and surface energy effects for samples of special shapes and sizes. For finite sized pentagonal samples, it is proposed that a phase transition between a vortex crystal and a vortex quasi-crystal occurs as a function of magnetic field and temperature as the sample size is reduced.

PACS numbers: 74.25.Op, 74.25.-q, 74.25.Dw

I. INTRODUCTION

The general subject of vortex physics in superconductors is quite interesting since there seems to be a large variety of possible equilibrium vortex phases in superconductors¹. The term “vortex matter” has been coined to emphasize the complexity and diversity of vortex phases in superconductors when compared to atomic and molecular matter. One can think of a one to one correspondence between phases in atomic and molecular matter (AMOM) and phases in vortex matter (VM). A liquid in AMOM corresponds to a vortex liquid in VM^{2,3}; a crystalline lattice in AMOM corresponds to a vortex lattice in VM⁴; an amorphous or glassy solid in AMOM corresponds to an amorphous or glassy vortex system in VM⁵. In addition, a quasi-crystal is another very interesting state which has been experimentally discovered in AMOM⁶, but there are no corresponding experiments for vortex matter.

The possibility of vortex quasi-crystals was initially discussed several years ago⁷, but more recently quasi-periodic arrangements of vortices were discussed in the presence of underlying quasiperiodic pinning potentials^{8,9,10,11}. In these recent theoretical and experimental studies it was suggested that the physical properties are quite unconventional due to the quasi-periodic pinning potentials. However, unlike these studies, the present paper is dedicated to a discussion of vortex quasi-crystalline phases in superconductors without quasi-periodic pinning potentials. This manuscript is an extension of our previous unpublished work^{7,12}, where it was argued that vortex quasi-crystals maybe stabilized by boundary effects and surface energies in finite systems. The present situation is quite distinct from the case of quasi-periodic pinning of vortices⁸ and from the case encountered in some atomic and molecular matter, where certain types of interactions can lead to colloidal quasi-crystals¹³.

The central question of this manuscript is: under what conditions a quasi-crystalline arrangement of vortices is at all possible? A definite possibility is to argue that a stable vortex quasi-crystal can arise from an imposed quasi-periodic potential like for instance in the case of a superconductor with quasi-periodic pinning potentials⁸,

or in heterostructures consisting of a superconductor film grown on top of a quasi-crystal film. Another possibility is to create a quasi-periodic optical lattice with laser beams, trap and cool atoms, and produce vortex quasi-crystals in Bose or Fermi superfluids. This experiment is natural since the production of vortex lattices in superfluid Bose or Fermi ultra-cold atoms has become standard^{14,15}, and more recently square optical lattices were used to induce transitions between triangular and square vortex lattices using a mask technique¹⁶. Thus, the generation of five-fold quasi-periodic optical lattices using a mask with five holes as the vertices of a regular pentagon (or other methods) may also be used to produce transitions between triangular and five-fold symmetric vortex lattices.

However, in this manuscript, we concentrate on the possibility of stabilizing vortex quasi-crystals only due to boundary effects in finite superconducting samples, where the sample size and shape play an important role. This option is motivated by recent experimental studies of the vortex structure in disk, triangular, square, and star-shaped mesoscopic samples^{17,18,19,20,21}. These works provide us with the technology that allows the preparation of pentagonal (pentagon-cylinders) or decagonal (decagonal-cylinders) samples as potential candidates to produce 5-fold vortex quasi-crystals. Furthermore, in these mesoscopic systems of cross-sectional area A , the number of vortices N is essentially given by $N = HA/\Phi_0$, where Φ_0 is the quantum of flux, and H is the magnetic field. Therefore samples with large upper critical field H_{c2} may produce a large enough number of vortices even the cross-sectional area is small, and the appearance of quasi-crystalline order is a definite possibility. For example, for a sample of cross sectional area $A = 1\mu\text{m}^2$ and upper critical field at zero temperature $H_{c2}(0) = 10\text{T}$, the number of vortices $N \approx 5000$ is quite substantial close to $H_{c2}(0)$. In addition, since superconductors with large H_{c2} are usually associated with short coherence lengths, the vortex quasi-crystalline phase proposed is more likely to be observable in proper samples of short coherence length superconductors at high magnetic fields and low temperatures.

This possibility is considered here under the following

program. In this manuscript only the case of an isotropic type II superconductor in a magnetic field is considered. First, the bulk free energy is calculated for a triangular, a square and a 5-fold quasi-crystal array. The 5-fold quasi-crystal array is modeled by a Penrose tiling of the plane as shown in Fig. 1. It is shown that the Penrose tile array (vortex quasi-crystal) has a bulk free energy which is just a few percent higher than the triangular array. Second, instead of considering an infinite (bulk) system, a pentagon cylinder sample is discussed. The pentagon cylinder has a pentagonal cross-section (in the xy plane) with side dimension ℓ , and with height L along the z direction. In this case, when the sample size gets smaller the contribution of the boundaries (surface energy) to the total free energy of the system becomes more important. The surface energy is highly sensitive to the symmetry and to the surface area of the boundaries. Taking into account the surface free energies, it is shown that the Penrose tiling (vortex quasi-crystal) has lower free energy than the triangular lattice in certain regions of the magnetic field versus temperature phase diagram. This is suggestive that a “first order phase transition” may occur between the triangular lattice and the Penrose tiling (vortex quasi-crystal)²².

The remainder of this manuscript is organized as follows. In section II, we discuss a Ginzburg-Landau approach to obtain the free-energy of the triangular, square and Penrose-tiling in the bulk. In section III, we present the effects of pentagonal boundaries on the free energy of the triangular lattice and Penrose-tiling, and obtain the critical magnetic field where the transition from triangular vortex lattice to a vortex quasi-crystal occurs. In section IV, we discuss thermodynamic quantities like the change in magnetization and entropy, while in section V, we discuss neutron scattering, Bitter decoration and scanning tunneling microscopy as possible probes to identify the quasi-crystalline structure. Lastly, in section VI we state our conclusions and summarize.

II. GINZBURG-LANDAU THEORY

The starting point of our analysis to describe the vortex-quasicrystal state is the Ginzburg-Landau (GL) free energy density

$$\Delta F_s = F_1 + \frac{1}{2m} \left| \left(-i\hbar\nabla - \frac{2e\mathbf{A}}{c} \right) \Psi(\mathbf{r}) \right|^2 + \frac{H^2}{8\pi} \quad (1)$$

for a bulk isotropic superconductor with no disorder, where $\Delta F_s = F_s - F_n$ is the free energy density difference between the superconducting state (F_s) and the normal state (F_n), and $F_1 = \alpha|\Psi(\mathbf{r})|^2 + \beta|\Psi(\mathbf{r})|^4/2$. It is useful to introduce the dimensionless quantities $f = \Psi\sqrt{-\beta/\alpha}$, $\boldsymbol{\rho} = \mathbf{r}/\lambda(T)$, $\mathcal{A} = 2\pi\xi(T)\mathbf{A}/\Phi_0$, and $\mathcal{H} = 2\pi\xi(T)\lambda(T)H/\Phi_0$, where λ is the penetration depth, ξ is the coherence length, and $\Phi_0 = hc/2e$ is the unit flux. Here, $f = f_0 \exp(i\phi)$, and $\mathcal{A} = \mathcal{A}_0 + \nabla\phi/\kappa$ with

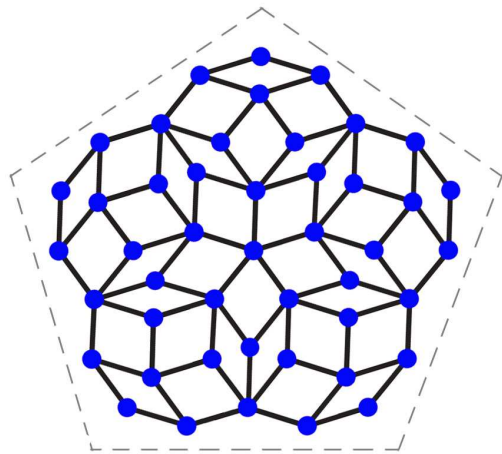


FIG. 1: We consider a vortex lattice in a pentagon superconducting sample having Penrose tiling with 5-fold rotational symmetry. The tile consists of two types of lozenges, one with internal angles 36° and 144° (thin lozenge) and the other with internal angles 72° and 108° (thick lozenge).

$\kappa = \lambda/\xi$ is the GL parameter. Notice that when $f_0 = 1$ the system is fully superconducting, and when $f_0 = 0$ the system is normal, thus $f_0 \leq 1$ always. Considering the minimization of free energy density with respect to \mathcal{A} and Ψ it is easy to arrive at equations for the dimensionless functions \mathcal{H} and f_0 . The microscopic field is

$$\mathcal{H}(x, y) = \kappa \left[1 + \frac{H - H_{c2}}{H_{c2}} \right] - \frac{g(x, y)}{2\kappa}, \quad (2)$$

with \mathbf{H} parallel to the z direction, and the equation for f_0 can be written as

$$\nabla^2(\log g) + 2\kappa^2 = 0, \quad (3)$$

where $g = f_0^2$ is a positive definite function. Notice that $\mathcal{H} = \kappa$ for $H = H_{c2}$ and $f_0 = 0$ ($g = 0$). The most general solution of Eq. (3) has the form²³

$$g(x, y) = \exp[-\kappa^2(x^2 + y^2)/2] \exp[\gamma(x, y)], \quad (4)$$

where $\gamma(x, y)$ satisfies Laplace's equation $\nabla^2\gamma(x, y) = 0$. This means that $\gamma(x, y)$ is a harmonic function excluding the locations of vortices, and can be expressed as the real part of an analytic function of $z = x + iy$. This observation has very important consequences for the microscopic field profile $\mathcal{H}(x, y)$ of Eq. (2), which depends strongly on the structure of $g(x, y)$.

The bulk Gibbs free energy density is given by⁴

$$G_s(H, T) = G_n(H, T) - \frac{1}{8\pi} \frac{(H_{c2} - H)^2}{(2\kappa^2 - 1)\beta}, \quad (5)$$

where the parameter $\beta = \langle g^2 \rangle / \langle g \rangle^2$ is a geometrical factor independent of κ . The notation $\langle \dots \rangle$ indicates average

over volume. It is important to notice that $\beta \geq 1$ no matter what is the form of $g(x, y)$ because of the Schwartz inequality. In addition, notice that the Gibbs free energy above is a minimum, whenever β reaches its minimum value.

For the purpose of calculating the parameter β and the free energies corresponding to different vortex configurations, the analytical structure of $g(x, y)$ in the complex plane is used to rewrite it as

$$g(z, \bar{z}) = \exp(-\kappa^2 z \bar{z}/2) |P(z)|, \quad (6)$$

where $P(z) = \mathcal{N} \prod_{i=1}^M (z - z_i)$. Here, each z_i corresponds to a zero of g in the complex plane, and M is the number of zeros. The zeros z_i indicate the location of vortices. From now on it is assumed that there is only one vortex with flux Φ_0 at each position z_i , i.e., each zero is non-degenerate. In this case, M corresponds to the number of vortices, and thus the total flux threading the sample is $\Phi = M\Phi_0$. The normalization coefficient \mathcal{N} just guarantees that $g(z, \bar{z}) \leq 1$. Depending on the locations of the zeros of $g(z, \bar{z})$, it is possible to study several possibilities of periodic and quasi-periodic vortex arrangements. In this study only vortex crystals corresponding to triangular and square lattices and vortex quasi-crystals corresponding to the 5-fold Penrose tiling of the plane are considered. Both the square lattices and triangular lattices can be generated via the tiling method, i.e., via the periodic arrangements of identical square tiles or identical lozenges of internal angles (60° and 120°). The Penrose lattice, however, requires quasi-periodic arrangements of two types of tiles (lozenges), one with internal angles 36° and 144° and the other with internal angles 72° and 108° . Using the representation in Eq. (6), the values of β for the triangular, square and Penrose tiling are respectively $\beta_3 = 1.16$, $\beta_4 = 1.18$ and $\beta_5 = 1.22$. This immediately indicates that the triangular lattice has lower free energy than the square lattice which has lower free energy than the 5-fold vortex quasi-crystal (Penrose tiling), as expected. However, the fact that the free energy difference between the triangular and 5-fold vortex quasi-crystal is only a few percent suggests that appropriate boundaries can favor 5-fold symmetry as the sample size gets smaller, as can appropriately imposed quasi-periodic potentials. Thus next, we discuss boundary effects and the magnetic field versus temperature phase diagram.

III. BOUNDARY EFFECTS AND PHASE DIAGRAM

In order to investigate how boundary effects can modify the total free energy of the system, a sample in the shape of a pentagon cylinder of side ℓ and height L is considered. Imposing that no currents flow through the sample boundaries leads to the condition

$$\hat{\mathbf{n}} \cdot [-i\nabla - 2\pi\mathbf{A}/\Phi_0] \Psi(x, y) = 0 \quad (7)$$

at all five side faces. The unit vector $\hat{\mathbf{n}}$ points along the normal direction of each facet of the pentagon cylinder. The boundary conditions can be translated in terms of the harmonic function $\gamma(x, y)$ as

$$n_x \frac{\partial \gamma}{\partial y} - n_y \frac{\partial \gamma}{\partial x} = \kappa(n_x y - n_y x), \quad (8)$$

where n_x and n_y are the x and y components of the normal unit vector $\hat{\mathbf{n}}$ at each one of the pentagon cylinder side faces. The solution for this boundary value problem can be obtained using a Schwarz-Christoffel conformal map of the pentagon into a semi-infinite plane

$$\frac{dz}{dw} = C(w - x_1)^{-2/5} (w^2 - x_2^2)^{-2/5} (w^2 - x_3^2)^{-2/5}, \quad (9)$$

where the vertices of the pentagon located at z_i are mapped into the points $(x_1, \pm x_2, \pm x_3)$ on the real axis of the w -plane. The full solution of this problem is complicated, and requires heavy use of numerical methods²⁴. However, the free energy density can be estimated when the bulk solution in Eq. (6) is treated as a variational solution of the boundary value problem determined by Eqs. (3), (8) and (9).

The Gibbs free energy density difference $\Delta G = G_3 - G_5$ between the triangular and the 5-fold quasi-periodic Penrose structure then becomes

$$\Delta G = -\frac{1}{8\pi} \frac{(H_{c2} - H)^2}{(2\kappa^2 - 1)\beta^*} + \frac{H_c^2}{4\pi} \epsilon(H), \quad (10)$$

where $\beta^* = \beta_3\beta_5/(\beta_5 - \beta_3)$, H_c is the thermodynamic critical field, and $\epsilon = (\alpha_3 - \alpha_5)(2R_e + \alpha_3 + \alpha_5)/2R_e^2$, with $\alpha_3 = 0.93a_0$, $\alpha_5 = 0.90a_0$, and $a_0 = \sqrt{\Phi_0/H}$. The effective length of the sample $R_e = \ell/\sqrt{4 - \tau^2}$, where $\tau = 2\cos(\pi/5)$ is the golden mean. Here, R_e corresponds to the radius of the circle that circumscribes the pentagonal sample.

This expression for ΔG is valid only when $H \gg \Phi_0/R_e^2$. The second term in ΔG takes into account the boundary mismatch energy, and indicates that as the size of the pentagon cylinder gets smaller it becomes more favorable to have a 5-fold quasi-crystal rather than a regular triangular lattice. Notice, however, that when $R_e \rightarrow \infty$ the triangular lattice has lower Gibbs free energy as it must, and no transition to a 5-fold quasi-crystal occurs. Thus, this possible transition may occur for finite sized samples only. From the condition that $\Delta G = 0$ we obtain

$$H_Q = H_{c2} \left[1 - \kappa^* \sqrt{\beta^* \epsilon(H_Q)} \right], \quad (11)$$

where the transition to a quasi-crystal occurs. Here, $\kappa^* = \sqrt{2\kappa^2 - 1}/\kappa$.

The phase diagram for a superconductor with $\kappa = 20$, $H_{c2}(0) = 10$ T and $R_e = 10^{-6}$ m is shown²⁵ in Fig. 2 using $H_{c2}(T) = H_{c2}(0) [1 - (T/T_c)^2]$. Notice that the number of vortices N close to H_Q can be quite large at low temperatures. For the parameters above $N =$

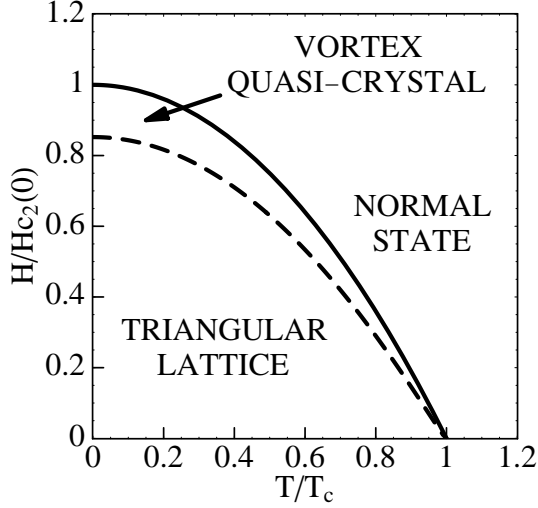


FIG. 2: $H - T$ phase diagram for a pentagonal cylinder cut out of a regular cylinder of radius for $R_e = 10^{-6}$ m. The solid and dashed lines represent H_{c2} and H_Q , respectively, while H_{c1} is not shown. The superconductor is assumed to have $\kappa = 20$, $H_{c2}(0) = 10$ T.

$H_Q A / \Phi_0 \approx 4000$, and the vortex quasi-crystal structure can be extracted. However, the phase diagram becomes less precise at high temperatures, since the low value of H sets a restriction on the number of vortices. Furthermore, for fixed $H_{c2}(0)$, one can find the critical value of $R_{e,c}$ below which the vortex quasi-crystal phase appears. Curves of $R_{e,c}$ versus T or H can be obtained and are shown in Fig. 3. Notice that the critical $R_{e,c}$ increases with increasing H (T) for a fixed T (H). Notice also that for a fixed sample size, and fixed magnetic field the vortex-quasi crystal phase always occurs at higher temperatures due to its higher entropy.

In order to address the signature of the crystal-quasicrystal phase transition, we discuss next thermodynamic properties including magnetization and entropy of the triangular and Penrose lattices in the pentagonal geometry.

IV. THERMODYNAMICS: CHANGES IN MAGNETIZATION AND ENTROPY

The jump of the magnetization $\Delta M (= M_3 - M_5)$ as a function of temperature at the critical field H_Q can be calculated from the Gibbs free energy leading to

$$\Delta M = \frac{H_{c2}}{4\pi} \left[-\frac{\gamma^*}{(2\kappa^2 - 1)\beta^*} + \Delta M_s \right], \quad (12)$$

where $\gamma^* = \kappa^* \sqrt{\beta^* \epsilon}$ and $\Delta M_s = (\alpha_3 - \alpha_5)(R_e + \alpha_3 + \alpha_5)/4\kappa^2 R_e^2 (1 - \gamma^*)$. A plot of ΔM is illustrated in Fig. 4 for the same parameters of Fig. 2. Using these parameters produces jump discontinuities $\Delta M \approx -0.060$ G at $T = 0$, and $\Delta M \approx -0.028$ G at $T = 0.8T_c$. However, measurements of ΔM may require the preparation

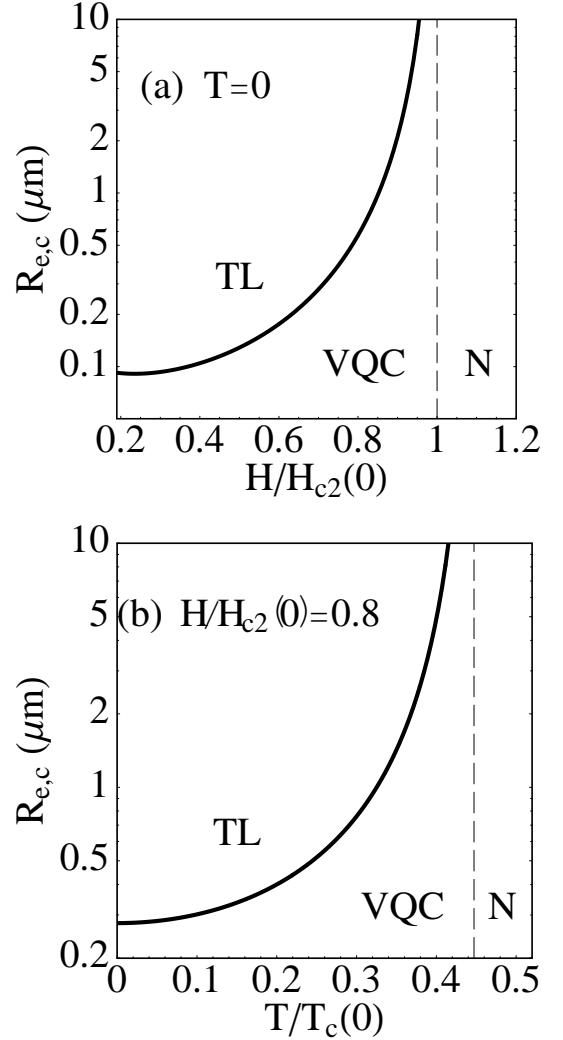


FIG. 3: Critical value of superconducting sample size $R_{e,c}$ as a function of (a) H for a given $T < T_c(0)$, and as a function of (b) T for a given $H < H_{c2}(0)$. Parameters used in these plots are the same as in Fig. 2, and the regions labeled TL, VQC, and N correspond to triangular lattice, vortex quasi-crystal, and normal phases, respectively.

of an array of identical pentagonal cylinders to enhance the overall value. Notice that $\Delta M < 0$ indicates that the 5-fold vortex quasi-crystal is denser than the triangular vortex lattice at H_Q , being at best a few percent denser at $T = 0$.

In addition to magnetization measurements, it is also interesting to perform calorimetric experiments. However, specific heat measurements are very difficult because they require large samples. Since sample size is important for the present discussion it is not clear that such experiments can be successfully performed. Nevertheless, the thermodynamic relationship between the magnetization and entropy jumps is revealed in the Clapeyron

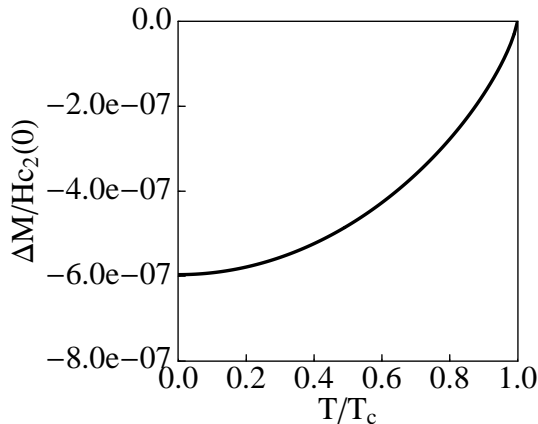


FIG. 4: The jump discontinuity $\Delta M = M_3 - M_5$ at the critical field H_Q for various reduced temperatures T/T_c , using the same parameters of Fig. 2.

equation

$$\Delta S = S_3 - S_5 = -\Delta M dH_Q/dT. \quad (13)$$

Since $dH_Q/dT < 0$, and $\Delta M < 0$ implies that $\Delta S < 0$, the entropy S_3 of the triangular vortex lattice is less than the entropy S_5 of the 5-fold vortex quasi-crystal, indicating that latent heat $L = T\Delta S$ is required to cause this phase transition.

Thermodynamic quantities can provide a good understanding of properties averaged over the entire sample, and can characterize the signature of the crystal-quasicrystal phase transition. However, as discussed above, a good measurement of these quantities may require an array of identical samples, which introduces experimental complexity and difficulty. As another possibility, the use of local probes discussed next is much desired in order to reveal the change in structure from a triangular vortex crystal to a 5-fold vortex quasi-crystal. For instance, neutron scattering, Bitter decoration or scanning tunneling microscopy (STM) experiments may help elucidate the structure of the vortex arrangement in mesoscopic samples.

V. LOCAL PROBES: NEUTRON DIFFRACTION AND SCANNING TUNNELING MICROSCOPY

In neutron diffraction experiments periodic or quasi-periodic variations of $\mathcal{H}(x, y)$ will result in Bragg peaks. The position of these peaks determine the characteristic length scale of the vortex structure and its symmetry. The neutron scattering amplitude in the Born approximation is

$$b(\mathbf{q}) = \frac{M_n}{2\pi\hbar^2} \int \mu_n H(\mathbf{r}) \exp(i\mathbf{q} \cdot \mathbf{r}) d\mathbf{r}, \quad (14)$$

where $\mu_n = 1.91e\hbar/M_n c$ is the neutron magnetic moment and the M_n is the neutron mass. The scattering

amplitude $b(\mathbf{q})$ is directly proportional to the Fourier transform $H(\mathbf{q})$ [$\mathcal{H}(q_x, q_y)$] of the microscopic field $H(\mathbf{r})$ [$\mathcal{H}(x, y)$] of Eq. (2). The neutron scattering cross section

$$\sigma(q_x, q_y) = 4\pi^2 |b(q_x, q_y)|^2 \quad (15)$$

has sharp peaks at $(q_x, q_y) = (0, 0)$ (central peak) and at $(q_x, q_y) = (\pm q_{xNm}, \pm q_{yNm})$ (first Bragg peaks), where $q_{xNm} = Q_N \cos(m\pi/N)$ and $q_{yNm} = Q_N \sin(m\pi/N)$, with $m = 0, 1, \dots, N-1$. For the triangular lattice $N = 3$ the first Bragg peak occurs at $|Q_3| = 2.31 \times \pi/d_3$, where d_3 is the lattice spacing. For the 5-fold vortex quasi-crystal (Penrose Lattice, $N = 5$) the first Bragg peak occurs at $|Q_5| = 2.46 \times \pi/d_5$, where d_5 is the side of a tile. Since the sample size is important for the observation of a 5-fold quasi-crystal, neutron scattering experiments may be difficult to perform.

However, Bitter decoration might be a useful technique if magnetic nanoparticles could be used to decorate the magnetic field profile, and then be seen by a scanning tunneling microscope (STM) (magnetic or non-magnetic). Furthermore, it may be possible to use just an STM to scan over the pentagonal sample and probe the local density of states which is substantially different inside and outside of vortex cores, due to the presence of vortex cores states. In this case, it may be also useful to make a periodic pattern of pentagonal samples, to obtain an ensemble average. It should be possible as well to perform STM scans at different fields and temperatures in the vicinity of $H_Q(T)$, which would reveal the real space locations of vortices. The pattern obtained could then be Fourier transformed (FT) to obtain a 6-fold pattern for the triangular vortex lattice and a 10-fold pattern for the 5-fold vortex quasi-crystal (Penrose lattice), which is shown in Fig. 5.

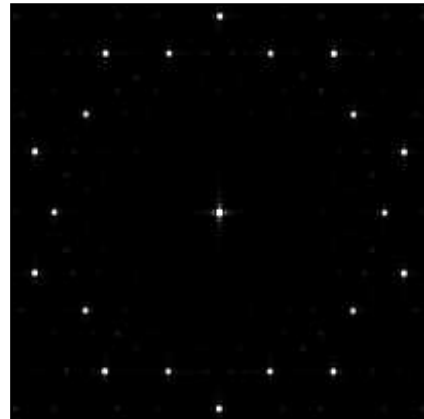


FIG. 5: First peaks of the square of the Fourier transformed (FT) pattern for the 5-fold vortex quasi-crystal (Penrose lattice). Notice that the pattern is 10-fold symmetric, unlike the case of the triangular vortex lattice, where the pattern is 6-fold symmetric.

Now that the phase diagram, thermodynamics, and the local signatures of a vortex quasi-crystal have been

discussed, it is important to say a word on the stability of such structures. A stability analysis in the free energy can be performed by moving the vortices away from their equilibrium positions z_i to $z_i + \delta z_i$. The eigenvalues associated with these displacements indicates that for $H > H_Q(T)$ the vortex quasi-crystal lattice is stable, and therefore potentially realizable in mesoscopic samples.

VI. FINAL COMMENTS AND CONCLUSIONS

Before concluding, we would like to make several comments in connection with the approximations used and the observability of the vortex quasi-crystal phase discussed.

First, it should be emphasized that our free energy analysis provides a preliminary understanding of the vortex quasi-crystal phase, but further detailed numerical work is necessary. For instance, the vortex quasi-crystal sitting on a Penrose lattice is only one possible state in a pentagon superconducting sample. Although we have shown that this state has lower free energy than a triangular or rectangular lattice, we cannot rule out other possibilities based on the present calculation.

Second, since there is no full compatibility of the 5-fold Penrose lattice with the pentagon cylinder geometry, the appearance of disclinations and dislocations is possible. As a result there is an additional possibility of a solid (crystal or quasi-crystal) vortex structure in the center of the sample, which melts or gets disordered at the sample boundaries²⁶.

Third, the number of vortices in superconducting samples is restricted by $N_{\max} = H_{c2}(0)A/\Phi_0$, which means that for superconductors with high H_{c2} a large number of vortices is possible. One can make a simple es-

timate for N_{\max} by using the Ginzburg-Landau relation $H_{c2} = \Phi_0/(2\pi\xi^2)$, leading to $N_{\max} \sim [R_e/\xi(T=0)]^2$. For conventional type II superconductors, the number N_{\max} is only about $10^1 \sim 10^2$, thus the thermodynamic limit and hence the definition of the quasi-crystal phase is questionable. However, for materials with short coherence length (and large upper critical fields), such as high- T_c superconductors, where $\xi(T=0)$ is about $10^1 \sim 10^2 \text{ \AA}$, then N_{\max} can be as large as $10^4 \sim 10^5$, and the quasi-crystalline structure can be well defined and observed. Thus, the observation of a vortex quasi-crystal state is more likely to occur in short coherence length superconductors at low temperatures and high magnetic fields.

Finally, strong disorder in the sample can also destroy the quasi-crystal structure due to the pinning of vortices, however, clean mesoscopic superconducting materials already exist and shell structures have been observed for Niobium samples of μm sizes²⁷. Thus, we suspect that experimentally this should not be an issue as vortex lattices (triangular) are routinely observed in reasonably clean superconducting samples. Therefore, the choice of pentagonal mesoscopic samples of superconductors with sufficiently large H_{c2} should allow for the observation of the vortex quasi-crystal state.

In summary, we have shown that vortex quasi-crystals may be experimentally observed in mesoscopic samples of type II superconductors with large upper critical fields (short coherence lengths). By taking into account boundary effects, sample shape and size, we proposed that a first order phase transition occurs between a vortex crystal and a vortex quasicrystal, as magnetic field and temperature are varied.

We would like to thank Wai Kwok and Franco Nori for references, the Aspen Center for Physics for their hospitality, and NSF (DMR-0304380) for financial support.

* Current address: Department of Physics, University of Michigan, Ann Arbor, Michigan, 48109.

¹ G. W. Crabtree and D. R. Nelson, *Physics Today* **50**(April), 38 (1997).

² H. Safar, P. L. Gammel, D. A. Huse, D. J. Bishop, W. C. Lee, J. Giapintzakis, and D. M. Ginsberg, *Phys. Rev. Lett.* **70**, 3800 (1993).

³ W. K. Kwok, J. Fendrich, S. Fleshler, U. Welp, J. Downey, and G. W. Crabtree, *Phys. Rev. Lett.* **72**, 1092 (1994).

⁴ A. A. Abrikosov, *Sov. Phys. JETP* **5**, 1174 (1957).

⁵ R. H. Koch, V. Foglietti, W. J. Gallagher, G. Koren, A. Gupta, and M. P. A. Fisher, *Phys. Rev. Lett.* **63**, 1511 (1989).

⁶ D. Shechtman, I. Blech, D. Gratias, and J. W. Cahn, *Phys. Rev. Lett.* **53**, 1951 (1984).

⁷ C. A. R. Sá de Melo, "Vortex Quasi-Crystals", manuscript no. LH7266, 05Aug99. See this unpublished work in cond-mat/0703156 (2007).

⁸ V. Misko, S. Sav'el'ev, and F. Nori, *Phys. Rev. Lett.* **95**, 177007 (2005); *Phys. Rev. B* **74**, 024522 (2006).

⁹ J. E. Villegas, M. I. Montero, C.-P. Li, and I. K. Schuller,

Phys. Rev. Lett. **97**, 027002 (2006).

¹⁰ M. Kemmler, C. Gurlich, A. Sterck, H. Pohler, M. Neuhaus, M. Siegel, R. Kleiner, and D. Koelle, *Phys. Rev. Lett.* **97**, 147003 (2006).

¹¹ A. V. Silhanek, W. Gillijns, V. V. Moshchalkov, B. Y. Zhu, J. Moonens, and L. H. A. Leunissen, *Appl. Phys. Lett.* **89**, 152507 (2006).

¹² Wei Zhang and C. A. R. Sá de Melo, cond-mat/0607624 (2006).

¹³ A. R. Denton and H. Lowen, *Phys. Rev. Lett.* **81**, 469 (1998).

¹⁴ M. R. Matthews, B. P. Anderson, P. C. Haljan, D. S. Hall, C. E. Wieman, and E. A. Cornell, *Phys. Rev. Lett.* **83**, 2498 (1999).

¹⁵ M. W. Zwierlein, J. R. Abo-Shaeer, A. Schirotzek, C. H. Schunck, and W. Ketterle, *Nature* **435**, 1047 (2005).

¹⁶ S. Tung, V. Schweikhard, and E. A. Cornell, cond-mat/0607697.

¹⁷ A. K. Geim, I. V. Grigorieva, S. V. Dubonos, J. G. S. Lok, J. C. Maan, A. E. Filippov, and F. M. Peeters, *Nature* **390**, 259 (1997).

- ¹⁸ A. K. Geim, S. V. Dubonos, J. J. Palacios, I. V. Grigorieva, M. Henini, and J. J. Schermer, Phys. Rev. Lett. **85**, 1528 (2000)
- ¹⁹ L. F. Chibotaru, A. Ceulemans, V. Bruyndoncx, and V. V. Moshchalkov, Nature **408**, 833 (2000); Phys. Rev. Lett. **86**, 1323 (2001).
- ²⁰ D. A. Dikin, V. Chandrasekhar, V. R. Misko, V. M. Fomin, and J. T. Devreese, Eur. Phys. J. B **34**, 231 (2003).
- ²¹ G. R. Berdiyorov, M.V. Milosevic, and F. M. Peeters, Phys. Rev. Lett. **96**, 207001 (2006).
- ²² The term “first order phase transition” appear in quotes since the sample size is finite.
- ²³ D. Saint-James, G. Sarma, and E. J. Thomas, *Type II superconductivity*, chap. 3, Pergamon Press, Oxford (1969).
- ²⁴ P. Henrici, *Applied and computational complex analysis*, vol III, chap. 16, John Wiley and Sons, New York (1986).
- ²⁵ The critical field $H_{c3}(T)$ for surface superconductivity is not shown in Fig. 2.
- ²⁶ L. R. E. Cabral, B. J. Baelus, and F. M. Peeters, Phys. Rev. B **70**, 144523 (2004).
- ²⁷ I.V. Grigorieva, W. Escoffier, J. Richardson, L.Y. Vinnikov, S. Dubonos, and V. Oboznov, Phys. Rev. Lett. **96**, 077005 (2006).